ISSN 1392-3730/eISSN 1822-3605

VILNIUS TECH
Vilnius Gediminas Technical University

JOURNAL of CIVIL ENGINEERING and MANAGEMENT

2024
Volume 30
Issue 8
Pages 758–766
https://doi.org/10.3846/jcem.2024.22302

PERFORMANCE-BASED DESIGN OF STRIP FOUNDATION CONSIDERING THE FULL EFFECT OF GROUND IMPROVEMENT

Yang YU[1], Xufei MAO[1], Mengfen SHEN[2]✉

[1] *Ocean College, Zhejiang University, Zhoushan, Zhejiang Province 316021, China*
[2] *College of Civil Engineering, Zhejiang University of Technology, Hangzhou 310014, China*

Article History:
- received 4 April 2024
- accepted 22 July 2024

Abstract. Ground improvement is an effective way to improve the bearing capacity of a shallow foundation. However, the benefit of reducing uncertainties in soil parameters for shallow foundation design is rarely recognized. This study investigated the full effect of rapid impact compaction (RIC) on a strip foundation design. The finite difference method coupled Monte Carlo simulation were used to calculate the failure probability and the required width of the strip foundation, where the friction angle of soil was treated as a random variable. The results show that the foundation width reduces by 48.5% when considering the full effect of RIC, and a significant part of the reduction came from the decrease in the uncertainty of friction angle. Although the adopted relationship between the friction angle and tip resistance of cone penetration test affects the designed width of the foundation, the full effect of ground improvement contributed by the uncertainty reduction of soil parameters is still significant. The implication of the present study provides a basis for the performance-based bearing capacity design of shallow foundations.

Keywords: foundation design, bearing capacity, coefficient of variation (COV), evaluation, uncertainty.

✉Corresponding author. E-mail: *mshen@zjut.edu.cn*

1. Introduction

The insufficient bearing capacity of a shallow foundation can result in shear or sliding damage, which can lead to the failure of the upper building. To address this issue, several ground improvement methods available to increase the foundation's bearing capacity. Some examples include dynamic compaction, rapid impact compaction, and the use of micropiles (Li et al., 2023). For a project site with loose deposits, ground improvement methods like dynamic compaction and rapid impact compaction (RIC) can be effective in increasing the densification, strength, and friction angle of the ground. This, in turn, enhances the bearing capacity of the shallow foundation (Mohammed et al., 2013; Tarawneh & Matraji, 2014). To evaluate the impact of ground improvement on the bearing capacity of the foundation, in situ tests such as cone penetration tests (CPT) are commonly conducted before and after the ground improvement process. These tests provide ways for assessing the effectiveness of the ground improvement in strengthening the soil resistance, which is of importance for the performance evaluation and optimal design of the shallow foundation.

In engineering practice, the magnitude of the CPT cone tips measured before and after the ground improvement are directly compared in order to qualitatively evaluate the effectiveness of ground improvement (e.g., Roslan, 2010; Bo et al., 2013; Eslami et al., 2015; Torrijo et al., 2017; Du et al., 2020). In order to quantitatively evaluate the effectiveness of ground improvement, the performances (e.g., the settlement or bearing capacity) of a shallow foundation before and after the ground improvement should be evaluated and compared (Yin et al., 2001; Mabrouki et al., 2010; Bouassida et al., 2015; Naseri & Hosseininia, 2015; Yahia-Cherif et al., 2017). Due to the presence of significant uncertainties in the ground conditions both before and after improvement, a reliability-based method is often adopted to evaluate the performance of shallow foundations. This approach takes into account the uncertainties associated with various parameters and provides a more comprehensive assessment of the foundation's reliability (Kayser & Gajan, 2014; Vahdatirad et al., 2015; Showkat & Babu, 2023). Reliability-based method has proven to be effective in investigating the bearing capacity and settle-

ment of shallow foundations. By considering uncertainties in various parameters, the approach provides a more robust and comprehensive evaluation of the foundation's performance (e.g., Fenton et al., 2007; Babu & Srivastava, 2007; Ahmed & Soubra, 2012; Wang et al., 2013; Yohanna et al., 2019).

Some researchers have noticed that the effects of ground improvement include two parts: increasing the shear strength of the ground and reducing the variability (uncertainty) of the soil properties (Shen et al., 2018, 2019). However, the full effect of ground improvement taking advantage of both benefits is rarely reported. Indeed, unless a design method explicitly considers the variability of the strength parameters, the full effect of ground improvement on the design (e.g., the size of the foundation) cannot be realized. Similar viewpoints have been reported in previous reliability-based studies (e.g., Shahin & Cheung, 2011; Shakir, 2019; Lakehal & Tiliouine, 2020).

In this study, we aim to highlight the full effect of ground improvement in a reliability-based (or performance-based) design of strip foundation. In the following sections, we first summarized the framework of reliability-based analysis to calculate the bearing capacity of the foundation. Then, based on the analysis method and framework, the effects of increasing soil strength and reducing the strength variability are examined through a case study. Furthermore, the influence of safety factors and conversion formula between friction angle and CPT data were discussed. Finally, the full effect of ground improvement in a foundation design is demonstrated. The results provide a basis for a performance-based design of shallow foundations taking advantage of an improved understanding of the full effect of ground improvement.

2. Methodology

2.1. The deterministic model for bearing capacity evaluation

FLAC 2D is used to solve the bearing capacity of a strip foundation, as shown in Figure 1. The boundary conditions of the model were set as follows. The *x*-velocities of the grid points on the symmetric plane were restricted. The *x*-velocities and *y*-velocities of the grid points on the bottom boundary and the right boundary were restricted. Due to the limited movement in the *x* and *y* directions of a bar foundation with a rough surface, it is necessary to set the speed of the grid to 0. The soil was modeled as a uniform Mohr-Coulomb material. To simulate the uniform load applied to the foundation, a vertical downward velocity was applied at the foundation position. The velocity must be sufficiently small to minimize the unbalanced force of the model. The fixed *x*-direction and *y*-direction grid points with zero velocities were used to simulate a strip foundation with a rough base surface. The number of zones along the vertical direction in the numerical model was determined based on the vertical interval of the CPT

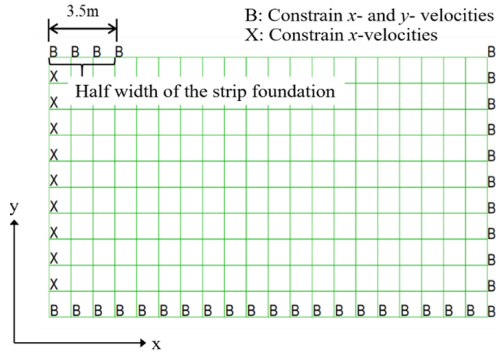

Figure 1. Simulation model for a strip foundation

data, computational efficiency and accuracy, which are illustrated in the case study presented later.

To substantiate the rationality of the adopted numerical model, specifically the model's boundary condition, the simulation of strip foundation and external load, a case study was conducted employing the FLAC2D software for calculation. In this case, the strip foundation with a rough surface was placed on soil, a uniformly distributed vertical load was applied on the foundation surface and half of the width of the strip foundation is 3.5 m. Refer to the reference (Erickson & Drescher, 2002), the unit weight of soil is 1700 kg/m^3, cohesion is 100 kPa, friction angle is 20°, shear module and volume module is 100 MPa and 200 MPa, respectively. The buried depth was assumed to be zero. In order to verify the accuracy of the numerical model, the bearing capacity of the strip foundation calculated by the FLAC 2D and the Terzaghi's theory were compared. The formula for the Terzaghi's ultimate bearing capacity theory is:

$$P_u = cN_c + qN_q + 0.5\gamma bN_\gamma, \quad (1)$$

where c is the cohesion of soil (kPa); γ is the unit weight of foundation soil (kg/m^3); q is the equivalent surcharge applied at the foundation bottom (kPa), which equals to the product of γ and foundation buried depth; b is the foundation width (m); N_c, N_q and N_γ are dimensionless bearing capacity factors that depend on the friction angle of the soil.

Figure 2 shows the calculated bearing capacities determined by the numerical modelling and the Terzaghi's theory. With the increase of time step, the bearing capacity calculated by the numerical modelling rises gradually. When the calculation time step exceeds 3700, the bearing capacity curve reaches its maximum value, that is, the ultimate bearing capacity of the strip foundation by the numerical modelling is 1.45×10^3 kPa. Compared to the ultimate bearing capacity by the Terzaghi's theory method, the error between these two methods is 0.97%, indicating the numerical modelling of FLAC 2D is reliable.

The displacement of foundation soil under strip foundation is shown in Figure 3. When the upper load reaches the ultimate bearing capacity of the foundation, the upper load continues to increase, resulting in the overall failure of the foundation. The velocity direction reflects the mov-

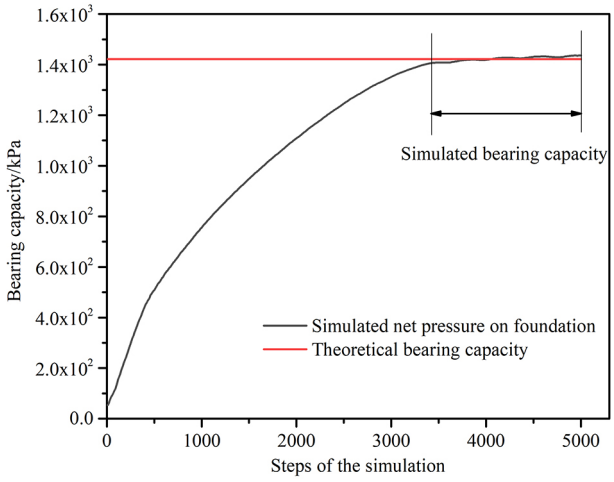

Figure 2. Baring capacity of the strip foundation

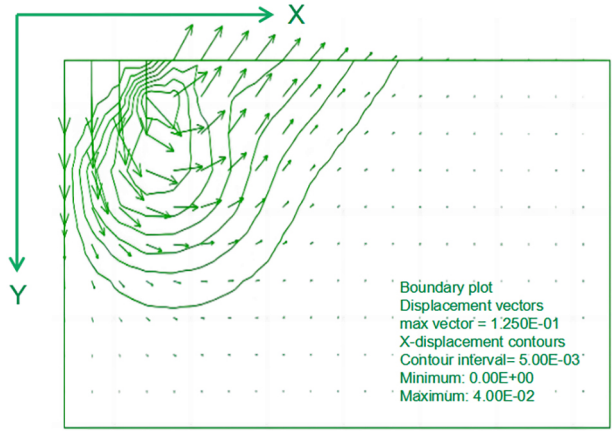

Figure 3. Displacement of foundation (Unit: m)

ing direction of the foundation soil, which is consistent with the theoretical failure mode proposed by Terzaghi, namely general shear failure.

2.2. Probabilistic evaluation of ground improvement

In reality, the geotechnical parameters are usually uncertain. For example, the friction angle value in one layer would vary from the other layer, and the value in one site would vary with the other site as well. Thus, the reliability analysis should be performed using, for example, Monte Carlo simulation (MCS) to consider the spatial variability of soil parameters. Then the probability of bearing capacity below its limit can be determined. Assuming the bearing capacity limit is denoted as B_L, the probability of bearing capacity below its limit is denoted as P_f, the performance function can be expressed as:

$$P_f = \frac{1}{N}\sum_{i=1}^{N} I(B_L - B_i), \quad (2)$$

where B_i is the bearing capacity calculated by the numerical model for the i_{th} realization. $I(B_L - B_i)$ is an indicator function, if $B_L - B_i > 0$, $I(B_L - B_i) = 0$, if $B_L - B_i \leq 0$, $I(B_L - B_i) = 1$.

As a rapid, easy, and reliable testing method, the cone penetration test receives much attention in geotechnical engineering. There are increasing empirical relationships built between the CPT and soil parameters. For example, friction angle φ can be estimated only by the tip resistance (q_c), which is referred to the Code for in-situ measurement of railway engineering geology (TB 10018-2003) (Ministry of Railways of the People's Republic of China, 2003):

$$\varphi = 29.609 * q_c^{0.0915}. \quad (3)$$

The benefits of ground improvement are illustrated from two perspectives: the reduction of damage risk caused by increasing the bearing capacity of the strip foundation, and the reduction of strip foundation cost. In this study, an engineering case was used to demonstrate the benefits of ground improvement. In this engineering case, the CPT data was used to evaluate the effectiveness of the ground improvement. The bearing capacity of the foundation was determined by the numerical modelling using FLAC 2D, and the spatial variability of friction angle was considered in this study. Three scenarios are considered. In scenario 1, the mean value (q_{cB}) and coefficients of variation (COV_B) of tip resistance before improvement were calculated based on field tests data. In scenario 2, the mean value (q_{cA}) of tip resistance after improvement was calculated based on field tests data. The COV of the tip resistance after improvement was assumed to be equal to COV_B. In scenario 3, the mean value (q_{cA}) and COV_A of tip resistance after improvement were calculated based on field tests data. In practice, COV_A is normally smaller than COV_B. The benefit of the ground improvement from the perspective of increasing the soil strength alone can be observed by comparing scenario 1 and scenario 2. On the other hand, the benefit of the ground improvement from the perspective of reducing the variation in the soil strength alone can be observed by comparing scenario 2 and scenario 3.

In the above three cases, the bearing capacity of the strip foundation needs to be calculated in order to obtain the failure probability. To calculate the bearing capacity of the strip foundation, the width of the strip foundation is needed. The probability that the bearing capacity of the strip foundation is below the bearing capacity limit shall be less than a certain value. If the width of the strip footing is fixed, the probabilities of the bearing capacity below its limit corresponding to the three scenarios can be obtained. On the other hand, if the acceptable probability of the bearing capacity below its limit of the strip foundation is specified, the footing width of scenarios 1, 2 and 3 can be back calculated according to the acceptable probability. Comparing with the footing width of scenario 1 and that of scenario 2, the benefit from the increase of soil strength is demonstrated. Comparing with the footing width of scenario 2 and that of scenario 3, the benefit from the decrease of variation in soil strength will be further demonstrated.

2.3. Framework

The framework to evaluate the full benefit of ground improvement is summarized as follows.

Step 1. Define the problem. Based on the soil type and purpose of the infrastructure, the allowable bearing capacity of the foundation and target reliability index (β) of the bearing capacity are determined firstly by the code. Specify the possible footing widths in discrete number *M* for selection.

Step 2. Collect CPT data before and after the ground improvement. Calculate the mean and COV value of the CPT data before and after ground improvement. Set the three scenarios defined in the Section 2.2.

Step 3. Establish the numerical model and determine proper zone numbers and size of elements. Establish the numerical model based on the defined problem in Step 1. In order to balance the efficiency and accuracy of numerical modelling, sensitive analyses of the element size are conducted to optimize the zone numbers and size of elements of the numerical model.

Step 4. Transform and characterize the CPT data. Based on the optimized size of elements, transform the original CPT data into new CPT data, whose interval is equal to the vertical size of the optimized elements of the numerical model. The mean value and COV of transformed CPT data are calculated to determine different scenarios.

Step 5. By substituting the CPT data into a conversion formula which established the relationship between CPT data and friction angle, the friction angle of soil layer is obtained. For each of the footing widths *M*, the Monte Carlo simulations are used to generate *N* groups of friction angle. The numerical model established in Step 3 is used to calculate the bearing capacity of the foundation corresponding to the *N* groups of friction angle, and thus the probability of the bearing capacity below its allowable value (P_f) is determined by Eqn (2). Repeat this process, obtain all the P_f of the *M* footing widths in these three scenarios.

Step 6. Evaluate the benefit from the decrease of variation in improved soil. Based on the target β, determine the optimal footing width (*B*). Comparing the design values of *B* in scenario 1 and in scenario 2 to demonstrate the benefit from the increase of the mean value of soil strength, and the tip resistance of CPT is used to represent the strength of soil. Comparing the design values of *B* in scenario 2 and in scenario 3 to further demonstrate the benefit from the decrease of variation in soil strength.

3. Illustrative example

3.1. Study project

The project selected as illustration was located at Sheik Mohammed Bin Zayed Road, Dubai, UAE (Tarawneh & Matraji, 2014). A total of 134 villas were constructed in the study area. Loose to very loose sand deposits were encountered at the depth ranging from 1.0 m to 4.5 m below the ground surface. To avoid damage to the villas, rapid impact compaction (RIC) was used to decrease the compatibility and increase the strength of the sand deposits. Due to lack of the foundation design information, the working load per unit area of the strip foundation was assumed as 500 kPa, and the safety factor was adopted by 3.0.

In the practice of ground improvement, the CPT are often conducted to evaluate the effectiveness of the RIC on the sand deposits by comparing the testing results (q_c) before and after the improvement. Figure 4 shows the tip resistance q_c of the 4 CPT tests as reported in Tarawneh and Matraji (2014). Figure 4a and Figure 4b show the q_c before and after the RIC, denoted as BRIC and ARIC, respectively. Focusing on the mean value (Figure 4c), it is observed that within the top 1.5 m, the disturbance of the top soil in the RIC process slightly decreases the strength.

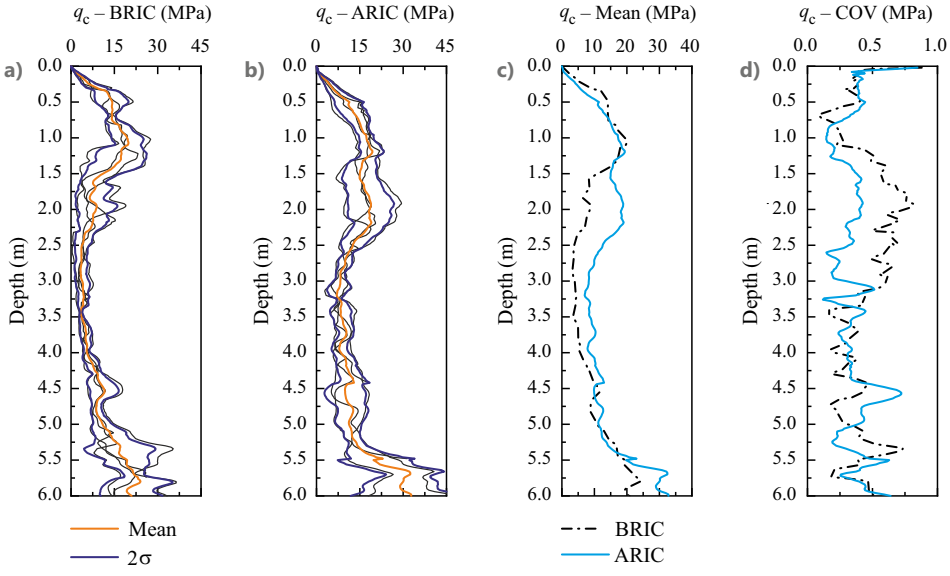

Figure 4. Statistics of q_c before and after RIC

From the depth of 1.5 m to 4.0 m, the increase in mean value of q_c is quite obvious, which means the influence depth of the RIC is from 1.5 m to 4.0 m at the 4 CPT test sites. Of particular interest in the plots of Figure 4d is the COV of the q_c values before and after the RIC. As shown in Figure 4(d), the COV of the q_c values after the RIC decrease significantly in the range of influence depth (from 1.5 m to 4.0 m). In the range of influence depth, the COV before and after the RIC are about 0.53 and 0.33, respectively.

3.2. Numerical model

In the numerical model for the study project, the unit weight was assumed as 1700 kg/m^3, the shear modulus was 100 MPa, and the volume modulus was 200 MPa, which were assigned based on the case in Figure 1. The cohesion was set as zero due to the cohesionless soil, and the friction angle was treated as a random variable estimated according to the CPT data (Eqn (3)). The friction angle varies along the depth direction. A representative value of the friction angle should be taken and assigned to the element of the numerical model. To get the representative value, the calculated friction angle within each layer of element were averaged then taken as the friction angle of the elements. In FLAC 2D, table command was used to assign the friction angle to the corresponding element. Then the bearing capacity of the strip foundation was calculated by considering the size of the strip foundation and other physical characteristics of the soil.

In order to determine the optimal element size and the number of elements, the influence of element size on the calculation of bearing capacity was investigated. The square shape of elements was used in the numerical model. The vertical size of the element was increased from 0.2 m to 1.2 m. Under the same base width, the mean value and COV of the bearing capacity corresponding to different vertical sizes of element are shown in Figure 5. When the vertical size of the element decreases from 1.2 m to 0.2 m, the bearing capacity of the strip foundation and the COV of the bearing capacity gradually decrease to a stable value. It can be observed that when the vertical size of the element is smaller than 0.5 m, the mean value and COV of the bearing capacity are not sensitive to variations in the element size. Therefore, to ensure both accuracy and efficiency of calculation, the optimal element size is determined to be 0.5 m.

The mean value and standard deviation of the tip resistance of each soil layer were measured at an interval of 0.5 m. The friction angle for each soil layer then were determined using the empirical relationship to the tip resistance q_c in Eqn (3). And then the mean value and standard deviation of friction angle for each soil layer were determined as input for the numerical simulation. The plastic constitutive model was adopted and the plastic modulus of each soil layer was assumed to be normally distributed. According to the normal distribution, the friction angle of each soil layer was generated randomly, and one realization is shown in the Figure 6.

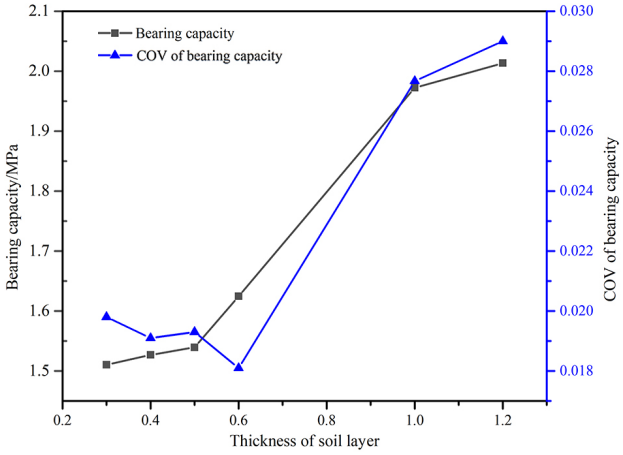

Figure 5. Bearing capacity and its COV of shallow foundations under different mesh sizes

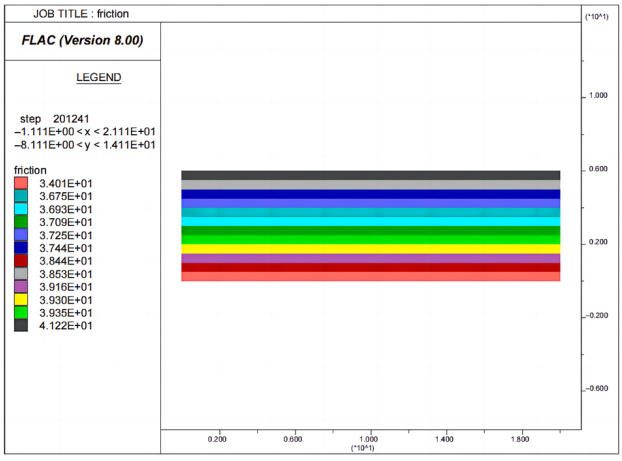

Figure 6. Friction angle for different soil layers (one realization)

3.3. Results

Recall that three scenarios of the mean values and COV are considered in this study. In Figure 7, the black curve represents the CPT data of scenario 1, the red curve represents the CPT data of scenario 2, and the blue curve represents the CPT data of scenario 3. At a depth of 6 m, every scenario's CPT data were divided into 12 soil layers by 0.5 m from top to bottom. The mean value and standard deviation of these different layers were then written into the command stream of FLAC 2D. The mean value of q_c of these 12 soil layers before the improvement are in the range of 3.54–21.35 MPa, and the standard deviation of these 12 soil layers are in the range of 0.26–4.95 MPa, respectively. The mean value of q_c after the improvement of these 12 soil layers are in the range of 4.66–28.67 MPa, and the coefficient of variation of the 12 soil layers is equal to the coefficient of variation of the 12 soil layers before improvement. In scenario 3, the mean value of q_c is equal to that in scenario 2, and the standard deviation of q_c of these 12 soil layers are in the range of 0.68–3.72 MPa. Comparing with scenario 1 and scenario 2 in Figure 7, it can be seen that the improvement significantly increases the mean value of q_c, which reflects the improvement of

soil strength after ground improvement. Comparing with scenario 2 and scenario 3 in Figure 7, it can be seen that the standard deviation of q_c is further reduced due to the improvement, which reflects the reduction in the variation of the soil strength after ground improvement. The mean value of CPT data in scenario 1, scenario 2, and scenario 3 are 10.09 MPa, 13.57 MPa, and 13.57 MPa, and COV of scenario 1, scenario 2, and scenario 3 are 0.58, 0.58 and 0.37. Using the Eqn (3), the mean value and COV of the friction angle in scenario 1, scenario 2 and scenario 3 can be determined, which are 36°, 37.3°, 37.2°, and 0.083, 0.079, and 0.046, respectively.

The failure probability was determined using the Monte Carlo simulation, which is the probabilities of the bearing capacity below its limit (500 kPa). In order to determine the proper number of MCS, the standard deviations of the calculated bearing capacity under the different number of MCS were determined. The results are shown in Figure 8. As the number of MCS increases, the standard deviation between the calculated results gradually decreases until it stabilizes and fluctuates slightly around a stable value. The standard deviation reaches a stable value when the number of MCS is 1200. Thus, the number of MCS is determined as 1200 considering the computational efficiency and accuracy.

Figure 9 shows the typical result of the MCS with the foundation width of 7 m. The y axis represents the allowable load per unit area of the foundation, which equals the ratio of the ultimate bearing capacity to the safety factor (= 3.0). There are 1200 simulations, 9 of which have an allowable load per unit area that is smaller than the limit value of 500 kPa. As a result, P_f = 9/1200 = 7.5×10^{-3}. The distribution of the allowable load per unit area under 1200 MCS is shown in Figure 10. It can be seen that it follows a normal distribution.

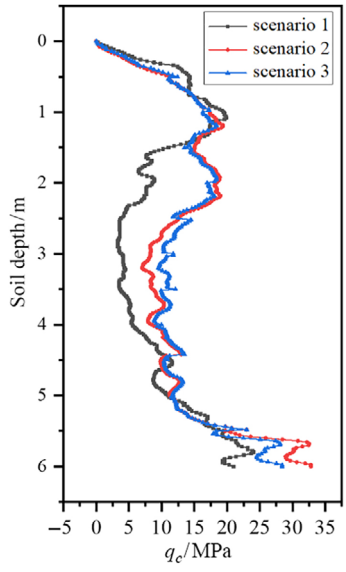

Figure 7. q_c of different scenarios

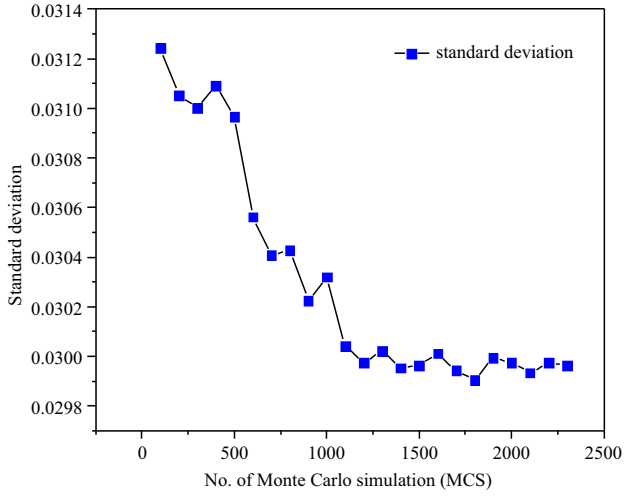

Figure 8. Standard deviation under different number of Monte Carlo simulation

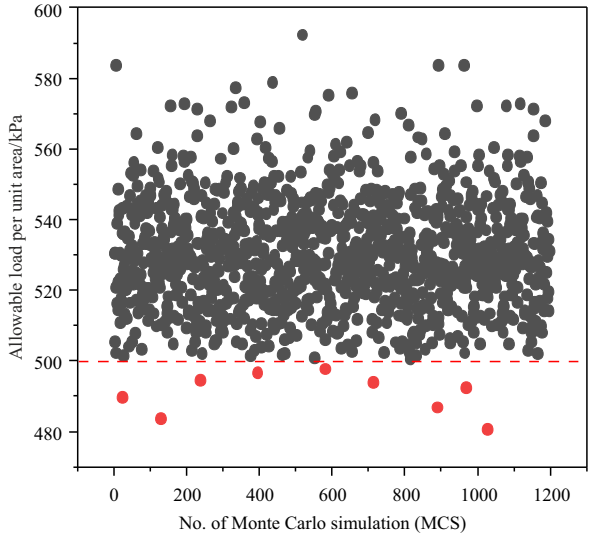

Figure 9. Scatter plot of Monte Carlo simulation results

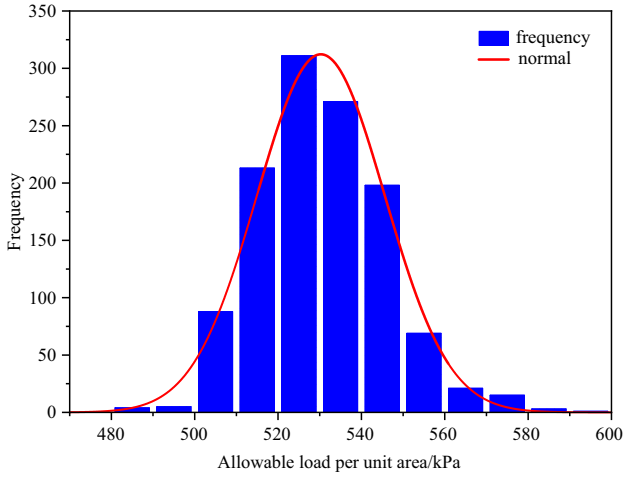

Figure 10. Histogram of the allowable load per unit area of the foundation

Under the foundation width of 7.0 m, the failure probabilities of scenario 1, scenario 2 and scenario 3 were calculated respectively (see Table 1). The failure probabilities of scenario 1, scenario 2 and scenario 3 are respectively 100%, 10.5% and approximately equal to 0. The reduction of failure probability means the increase of the bearing capacity of shallow foundation. In other words, under the condition that the width of the shallow foundation is unchanged, the bearing capacity of the shallow foundation can be improved by considering the full effect, thus reducing the failure probability of the foundation.

With the calculated P_f, the reliability index (β) then can be determined using the relationship $P_f = \Phi(-\beta)$. To find the minimum foundation width that satisfies the target reliability index, numerous trial calculations were conducted. First, the P_f for a shallow foundation with a specified width was determined using the methodology described above. Then, the β was calculated based on the P_f. If the calculated β was greater than the target β, the foundation width was reduced; otherwise, the foundation width was increased. By repeating this process, two critical values of foundation width were identified through extensive trial calculations, and the minimum foundation width that meets the target reliability index will fall within this range, as shown in Figure 11.

In Figure 11, the line corresponding to the two critical foundation widths are intersected with the line of the target reliability index, and the foundation width corresponding to the intersection point is the minimum foundation width which satisfying the target β. Assuming the target β is 3.0 for a strip foundation, the foundation width for scenario 1, scenario 2, and scenario 3 is 6.17 m, 3.73 m, and 3.18 m, respectively. Comparing scenario 1 with scenario 2, the width of the shallow foundation decreases by 2.44 m when increasing friction angle from 36° to 37.3°. Comparing with scenario 2 and scenario 3, the width of the shallow foundation is further reduced by 0.55 m caused by reducing the variation of friction angle from 0.079 to 0.046. In other words, the foundation width reduces 48.5% (= 100% × 2.99/6.17) when considering the full effect of ground improvement, and the 18.4% (= 100% × 0.55/2.99) is contributed by variation reduction of friction angle, which is not negligible.

Table 1. Effects of ground improvement on failure probability (footing width is 3.5 m)

Scenario	Description	q_c	COV of q_c	P_f
1	Unimproved sand	S1 in Figure 7	0.58	100%
2	Improved soil without reduction in COV	S2 in Figure 7	0.58	10.5%
3	Improved soil with reduction in COV	S3 in Figure 7	0.37	≈0%

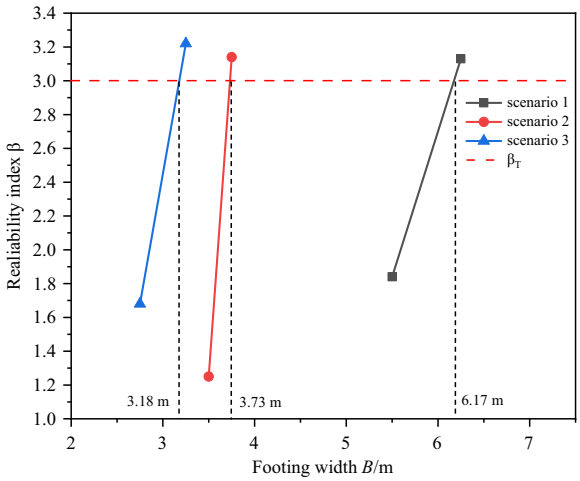

Figure 11. The width of shallow foundations under different scenarios

4. Discussion

4.1. Influence of safety factor

To further investigate the benefit from the decrease of the COV, different safety factor was considered. In addition, focus on the foundation widths required by scenarios 2 and scenarios 3. The previous safety factor is 3.0, now the safety factor is increased to 3.2, 3.4, 3.6. Then, the method described above was used to calculate the foundation widths required by scenario 2 and scenario 3 under different safety factors, respectively. The required width of strip foundation corresponding to different safety factors is shown in Figure 12. When the safety factor is increased to 3.2, 3.4 and 3.6, the foundation width required by scenario 3 is reduced by 0.75 m, 0.58 m and 0.60 m respectively compared with that required by scenario 2.

Overall, the benefits brought by scenario 3 are relatively similar under different safety factors. Furthermore, according to the analysis of the Terzaghi's formula and the

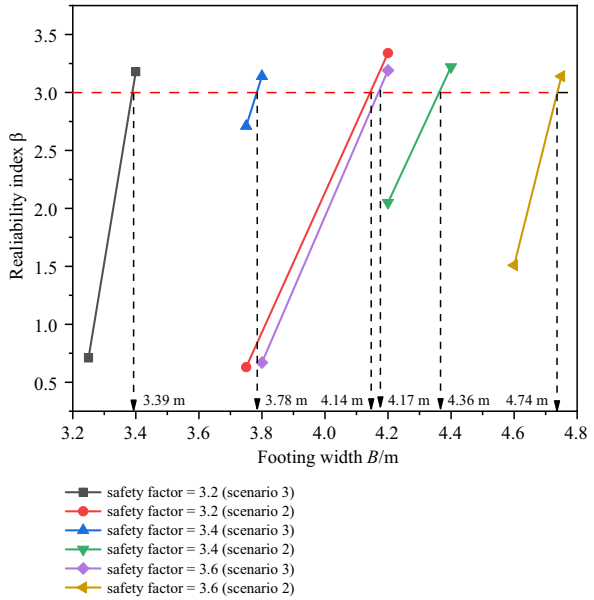

Figure 12. Effect of changing safety factor on width of shallow foundations

generation process of random number, when the COV of the strength of the soil under the foundation is constant, improving the safety factor of the foundation cannot enhance or weaken the optimization effect of the foundation size brought by the reduction of COV.

4.2. Influence of conversion formula

The other conversion formulas between the soil's friction angle and the tip resistance of the CPT can be found in Lin et al. (2018), and the formula is:

$$\varphi = -0.0075q_c^2 + 0.6072q_c + 32.58. \quad (4)$$

The calculation results are then shown in the Figure 13. In this case, the foundation width required by scenario 2 is 3.73 m, and that required by scenario 3 is 3.22 m, with a 0.51 m reduction in width, and the foundation size is further optimized. It shows different widths may be designed using different conversion formulas between friction angle and tip resistance, but the optimization effect of reducing COV on foundation width is still applicable.

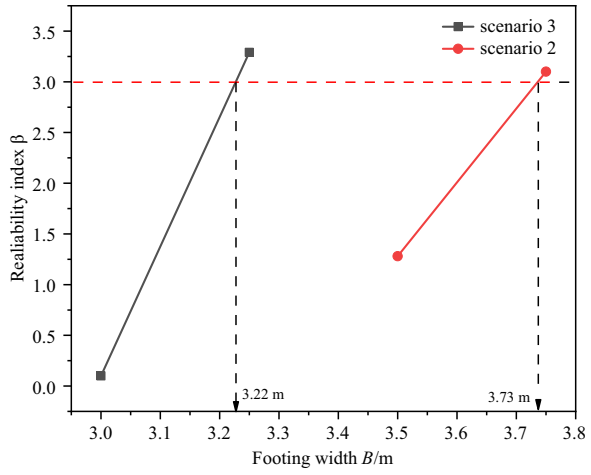

Figure 13. Designed width of shallow foundations under scenario 2 and scenario 3 by correlation relation proposed by Lin et al. (2018)

5. Conclusions

Based on the concept of reliability design in geotechnical engineering, the full effect of ground improvement on the shallow foundation design was evaluated. It can be concluded that:

(1) The effect of rapid impact compaction on the shallow foundation design is from two aspects: the increase in friction angle and the reduction in the variation of the friction angle. These two effects should be fully considered as the later effect is not negligible in the reliability design of foundation.

(2) In this study, the foundation width reduces 48.5% when considering the full effect of ground improvement, and 18.4% of the reduction is contributed by the variation decrease of friction angle.

(3) The influence of safety factor and conversion formula on the size of foundation were investigated. The minimum foundation width increases with the increase of the safety factor while the reliability index stays unchanged. Similarly, different conversion formulas require different minimum foundation widths. In both cases, the full effect of ground improvement is still significant for reducing the foundation size.

It should be noted that these conclusions are based on limited data. The exact value may be different in other examples. However, the comparative study is still valid to investigate the effect of uncertainty reduction in soil parameter due to ground improvement on the foundation engineering design. It demonstrates that current approaches, which focus mainly on increased soil strength, often do not fully utilize the benefits of soil improvement, such as the significant reduction in soil variability. This is significant in engineering practice, as it provides a basis for performance-based or risk-based foundation design to mitigate the risk of damage or failure due to insufficient bearing capacity of shallow foundations.

Acknowledgements

The authors wish to acknowledge the financial support from the National Natural Science Foundation of China (42277129, 42007236), the Fundamental Research Funds for the Central Universities (226-2024-00197) and the Zhejiang Provincial National Science Foundation of China (LR24E080004, LY24D020001).

References

Ahmed, A., & Soubra, A. H. (2012). Probabilistic analysis of strip footings resting on a spatially random soil using subset simulation approach. *Georisk*: *Assessment and Management of Risk for Engineered Systems and Geohazards*, *6*(3), 188–201. https://doi.org/10.1080/17499518.2012.678775

Babu, G. L. S., & Srivastava, A. (2007). Reliability analysis of allowable pressure on shallow foundation using response surface method. *Computers and Geotechnics*, *34*(3), 187–194. https://doi.org/10.1016/j.compgeo.2006.11.002

Bo, M. W., Arulrajah, A., Horpibulsuk, S., Leong, M., & Disfani, M. M. (2013). Densification of land reclamation sands by deep vibratory compaction techniques. *Journal of Materials in Civil Engineering*, *26*(8), Article 06014016. https://doi.org/10.1061/(ASCE)MT.1943-5533.0001010

Bouassida, M., Jellali, B., & Lyamin, A. (2015). Ultimate bearing capacity of a strip footing on ground reinforced by a trench. *International Journal of Geomechanics*, *15*(3), Article 06014021. https://doi.org/10.1061/(ASCE)GM.1943-5622.0000418

Du, G., Xia, H., Cai, J., Pan, H., & Sun, C. (2020). Liquefiable ground treatment using cruciform section probe resonant compaction method: A case study in the Xitong Expressway, Eastern China. *Advances in Civil Engineering*, *2020*, Article 6564193. https://doi.org/10.1155/2020/6564193

Erickson, H. L., & Drescher, A. (2002). Bearing capacity of circular footings. *Journal of Geotechnical and Geoenvironmental Engineering*, *128*(1), 38–43. https://doi.org/10.1061/(ASCE)1090-0241(2002)128:1(38)

Eslami, A., Pirouzi, A., Omer, J. R., & Shakeran, M. (2015). CPT-based evaluation of Blast Densification (BD) performance in loose deposits with settlement and resistance considerations.

Geotechnical and Geological Engineering, *33*(5), 1279–1293. https://doi.org/10.1007/s10706-015-9900-x

Fenton, G. A., Zhang, X., & Griffiths, D. V. (2007). Reliability of shallow foundations designed against bearing failure using LRFD. *Georisk Assessment and Management of Risk for Engineered Systems and Geohazards*, *1*(4), 202–215. https://doi.org/10.1080/17499510701812844

Kayser, M., & Gajan, S. (2014). Application of probabilistic methods to characterize soil variability and their effects on bearing capacity and settlement of shallow foundations: state of the art. *International Journal of Geotechnical Engineering*, *8*(4), 352–364. https://doi.org/10.1179/1938636213Z.00000000073

Lakehal, S., & Tiliouine, B. (2020). Safety assessment of shallow foundations resting on sandy soils with correlated parameters. *Arabian Journal for Science and Engineering*, *45*(5), 3829–3841. https://doi.org/10.1007/s13369-019-04264-0

Li, Y. X., David, A., & Feng, W. Q. (2023). Effectiveness of rolling dynamic compaction with a three-sided compactor on unsaturated sand. *Transportation Geotechnics*, *42*, Article 101093. https://doi.org/10.1016/j.trgeo.2023.101093

Lin, Z. H., Feng, T., Meng, S. W., & Li, C. H. (2018). Study on the relevance between angle of internal friction and cone resistance. *Chinese Journal of Underground Space and Engineering*, *S2*, 639–644 (in Chinese).

Mabrouki, A., Benmeddour, D., Frank, R., & Mellas, M. (2010). Numerical study of the bearing capacity for two interfering strip footings on sands. *Computers and Geotechnics*, *37*(4), 431–439. https://doi.org/10.1016/j.compgeo.2009.12.007

Ministry of Railways of the People's Republic of China. (2003). *Code for in-situ measurement of railway engineering geology* (TB 10018-2003).

Mohammed, M. M., Roslan, H., & Firas, S. (2013). Assessment of rapid impact compaction in ground improvement from in-situ testing. *Journal of Central South University*, *20*(3), 786–790. https://doi.org/10.1007/s11771-013-1549-0

Naseri, M., & Hosseininia, E. S. (2015). Elastic settlement of ring foundations. *Soils and Foundations*, *55*(2), 284–295. https://doi.org/10.1016/j.sandf.2015.02.005

Roslan, H. (2010). Effective improvement depth for ground treated with rapid impact compaction. *Scientific Research and Essays*, *5*(18), 2686–2693.

Shahin, M., & Cheung, E. M. (2011). Probabilistic analysis of bearing capacity of strip footings. In *Geotechnical Safety and Risk*. *ISGSR*, 2011 (pp. 225–230).

Shakir, R. R. (2019). Probabilistic-based analysis of a shallow square footing using Monte Carlo simulation. *Engineering Science and Technology*, *22*(1), 313–333. https://doi.org/10.1016/j.jestch.2018.08.011

Shen, M., Martin J. R., Ku, C.-S., & Lu, Y.-C. (2018). A case study of the effect of dynamic compaction on liquefaction of reclaimed ground. *Engineering Geology*, *240*, 48–61. https://doi.org/10.1016/j.enggeo.2018.04.003

Shen, M., Juang, C. H., Ku, C.-S., & Khoshnevisan S., (2019). Assessing effect of dynamic compaction on liquefaction potential using statistical methods – a case study. *Georisk*: *Assessment and Management of Risk for Engineered Systems and Geohazards*, *13*, 341–348. https://doi.org/10.1080/17499518.2019.1623407

Showkat, R., & Babu, G. L. S. (2023). Deterministic and probabilistic analysis of the response of shallow footings on unsaturated soils due to rainfall. *Transportation Geotechnics*, *43*, Article 101150. https://doi.org/10.1016/j.trgeo.2023.101150

Tarawneh, B., & Matraji, M. (2014). Ground improvement using rapid impact compaction: case study in Dubai. *Građevinar*, *66*(11), 1007–1014.

Torrijo, F. J., Garzón-Roca, J., Alija, S., & Quinta-Ferreira, M. (2017). Dynamic compaction evaluation using in situ tests in Sagunto's Harbor, Valencia (Spain). *Environmental Earth Sciences*, *76*(19), Article 658. https://doi.org/10.1007/s12665-017-7033-7

Vahdatirad, M. J., Bayat, M., Andersen, L. V., & Ibsen, L. B. (2015). Probabilistic finite element stiffness of a laterally loaded monopile based on an improved asymptotic sampling method. *Journal of Civil Engineering and Management*, *21*(4), 503–513. https://doi.org/10.3846/13923730.2014.890660

Wang, Y., Zhao, X., & Wang, B. (2013). LS-SVM and Monte Carlo methods based reliability analysis for settlement of soft clayey foundation. *Journal of Rock Mechanics and Geotechnical Engineering*, *5*(4), 312–317. https://doi.org/10.1016/j.jrmge.2012.06.003

Yin, J. H., Wang, Y. J., & Selvadurai, A. P. S. (2001). Influence of nonassociativity on the bearing capacity of a strip footing. *Journal of Geotechnical and Geoenvironmental Engineering*, *127*(11), 985–990. https://doi.org/10.1061/(ASCE)1090-0241(2001)127:11(985)

Yahia-Cherif, H., Mabrouki, A., Benmeddour, D., & Mellas, M. (2017). Bearing capacity of embedded strip footings on cohesionless soil under vertical and horizontal loads. *Geotechnical and Geological Engineering*, *5*(2), 547–558. https://doi.org/10.1007/s10706-016-0124-5

Yohanna, P., Oluremi, J. R., Eberemu, A. O., Osinubi, K. J., & Sani, J. E. (2019). Reliability assessment of bearing capacity of cement-iron ore tailing blend black cotton soil for strip foundations. *Geotechnical and Geological Engineering*, *37*(2), 915–929. https://doi.org/10.1007/s10706-018-0660-2